Chemistry & Biology, Vol. 10, 769–778, August, 2003, ©2003 Elsevier Science Ltd. All rights reserved. DOI 10.1016/S1074-5521(03)00173-X

Structural Basis for Contrasting Activities of Ribosome Binding Thiazole Antibiotics

Georg Lentzen,[1,3] Roscoe Klinck,[1,2] Natalia Matassova,[1] Fareed Aboul-ela,* and Alastair I.H. Murchie
RiboTargets, Ltd.
Granta Park
Abington, Cambridge CB1 6GB
United Kingdom

Summary

Thiostrepton and micrococcin inhibit protein synthesis by binding to the L11 binding domain (L11BD) of 23S ribosomal RNA. The two compounds are structurally related, yet they produce different effects on ribosomal RNA in footprinting experiments and on elongation factor-G (EF-G)-dependent GTP hydrolysis. Using NMR and an assay based on A1067 methylation by thiostrepton-resistance methyltransferase, we show that the related thiazoles, nosiheptide and siomycin, also bind to this region. The effect of all four antibiotics on EF-G-dependent GTP hydrolysis and EF-G-GDP-ribosome complex formation was studied. Our NMR and biochemical data demonstrate that thiostrepton, nosiheptide, and siomycin share a common profile, which differs from that of micrococcin. We have generated a three-dimensional (3D) model for the interaction of thiostrepton with L11BD RNA. The model rationalizes the differences between micrococcin and the thiostrepton-like antibiotics interacting with L11BD.

Introduction

The bacterial ribosome is the main target for several classes of antibiotics. With the elucidation of the X-ray structures of 30S, 50S, and 70S ribosomes [1–4], our understanding of the mode of action of many ribosome binding antibiotics, including the aminoglycosides, tetracyclines, and macrolides, has advanced (for reviews, see [5, 6]). However, the interaction of thiazole antibiotics with the ribosome remains unknown. Micrococcin and thiostrepton are the best-studied members of this group and act by binding in the region around position 1067 in 23S rRNA. This is also the site at which ribosomal proteins L11 and L10-$(L7/L12)_2$ are bound [7, 8]. We term this RNA region the L11 binding domain, L11BD (Figure 1A). Elongation factor G (EF-G), a GTPase that hydrolyses GTP on the ribosome and promotes translocation, also interacts with this region [9–11]. Both drugs interfere with EF-G function on the ribosome [12–15].

There are multiple lines of evidence that thiostrepton and micrococcin act by binding to rRNA and contact L11, yet there are subtle differences in their interactions with the ribosome. Mutations at A1067 confer resistance to thiostrepton [16]. Both drugs protect A1095 from chemical modification, but reactivity by DMS at A1067 is reduced by thiostrepton and increased by micrococcin [16–18]. Thiostrepton binding to the 1067 region is stimulated by L11 [19]. L11-deficient mutants show a decreased sensitivity toward thiostrepton and micrococcin [20, 21]. On the other hand, EF-G-dependent GTP hydrolysis is inhibited by thiostrepton and enhanced by micrococcin [21, 22].

Thiostrepton binds to a L11BD oligonucleotide (Figure 1A) and to 23S rRNA with a similar affinity ($K_d \sim 10^{-6}$ M) [23]. The L11BD can fold independently, and high-resolution X-ray structures of this RNA complexed with the entire L11 protein [24] or its C-terminal domain [25] have been solved. The structures reveal a complex tertiary fold in which residues 1067 and 1095 are in proximity. However, no thiazole-bound structure has been reported. In fact, the poor aqueous solubility of the thiazoles has been a hindrance to structural studies. In this paper, we have used thiostrepton-resistance (TSR) methyltransferase from *Streptomyces azureus*, the producer of thiostrepton, as a probe for the interaction of thiazole antibiotics with L11BD. 2′O-methylation of A1067 by this enzyme renders ribosomes resistant to thiostrepton [13, 21]. We have used the interference of thiazoles with A1067 methylation to probe their interaction with L11BD. We have obtained a soluble thiostrepton-L11BD RNA complex that is suitable for NMR studies. We have identified intermolecular NOEs in this complex, allowing us to model the interaction between thiostrepton and L11BD. We show that the related thiazole antibiotics nosiheptide and siomycin interact with L11BD in a manner similar to that of thiostrepton and in contrast to that of micrococcin. These findings parallel differential effects on EF-G-dependent reactions for the four thiazole compounds. We propose a 3D model for thiostrepton binding to L11BD which is consistent with the NMR and methylation data and explains the striking similarities and differences in the biochemical effects of these thiazole antibiotics on L11BD.

Results

We first verified the biological activities of four thiazole antibiotics known to act as translational inhibitors: thiostrepton, micrococcin, siomycin, and nosiheptide. Indeed, all four are potent inhibitors of bacterial translation with greater than 100-fold selectivity over the inhibition of eukaryotic translation (Table 1). The inhibition seen in the coupled transcription/translation system was confirmed in an uncoupled assay using MS2 phage RNA as mRNA and measuring the inhibition of incorporation of [^{35}S]methionine (data not shown).

L11 and Thiazole Binding Block Methylation by TSR Enzyme

TSR methyltransferase from *Streptomyces azureus* was used to characterize the binding of the thiazoles to

*Correspondence: f.aboul-ela@ribotargets.com
[1] These authors contributed equally to this work.
[2] Present address: Département de Microbiologie et d'Infectiologie Faculté de Médecine, Université de Sherbrooke, Sherbrooke, Quebec J1H 5N4, Canada.
[3] Present address: Bitop AG, Stockumer Strasse 28, 58453 Witten, Germany.

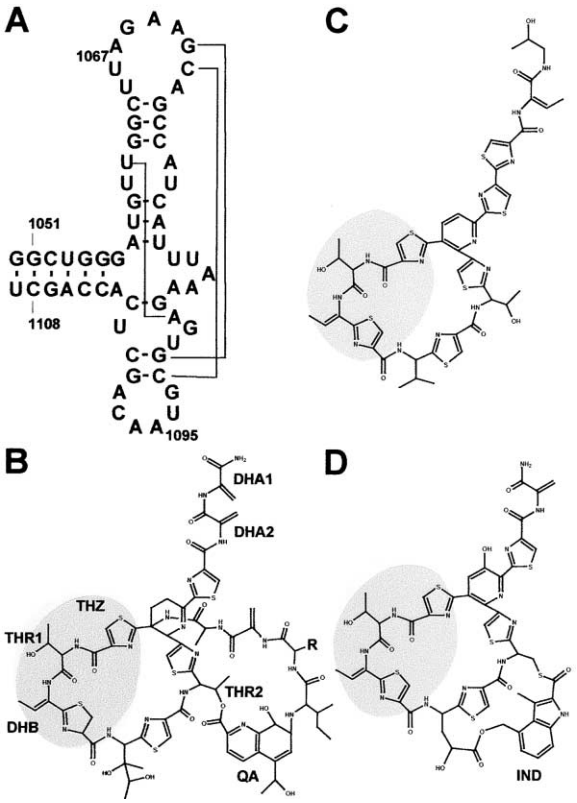

Figure 1. L11BD RNA and Thiazole Antibiotics

(A) Secondary structure of the L11BD RNA construct representing nucleotides 1051 to 1108 (*E. coli* numbering) of *Thermatoga maritima* 23S rRNA. Watson-Crick base pairings are indicated as dashes, and key tertiary interactions observed in the crystal structure are shown as thin lines. An additional G-U base pair was introduced on the 5′ end of this construct to improve the in vitro transcription yield.

(B–D) Chemical structures of thiostrepton (R = CH_2) and siomycin (R = CH_3) (B), micrococcin (C), and nosiheptide (D). For thiostrepton, dehydrobutyrine (DHB), quinaldic acid (QA), thiazole (THZ), threonines (THR1, 2), and dehydroalanines (DHA1, 2) residues referred to in the text are labeled. The indole (IND) moiety on nosiheptide is labeled. Gray shading highlights the conserved substructure among this group of antibiotics.

L11BD by measuring the transfer of methyl groups from S-adenosyl-L-methyl-[^{3}H]methionine ([^{3}H]SAM). Ribosomal RNA from *E. coli* and the L11BD construct were tested for their susceptibility to modification by TSR methyltransferase in vitro. Both were efficiently methylated by the enzyme with K_m values of ~30 nM and ~50 nM, respectively (Figure 2A). Control experiments showed that methylation is specific for the L11BD sequence. For example, a 30 nucleotide RNA representing the TAR domain of HIV and a 78 nucleotide construct containing residues 2107–2182 of *E. coli* 23S rRNA (the L1 protein binding site) were not methylated by TSR methyltransferase, even at 50 μM RNA.

L11 inhibits methyltransferase activity [26]. As shown in Figure 2B, increases in L11 concentration inhibited L11BD methylation. The measured inhibition constant K_i = 120 nM is in agreement with affinity determinations by nitrocellulose filter binding (K_d = 90nM, [27]).

The binding of thiostrepton to 23S rRNA or L11BD

Table 1. Inhibition of Translation by Thiazole Antibiotics

	IC_{50} (μM) *(E. coli)*	IC_{50} (μM) (Rabbit Reticulocyte)
Thiostrepton	0.10 ± 0.01	>200
Siomycin	0.25 ± 0.04	>200
Nosiheptide	0.23 ± 0.06	>200
Micrococcin	0.30 ± 0.01	>100

The inhibition constant (IC_{50}) was obtained from concentration-response curves as the concentration of half-maximal inhibition in a coupled *E. coli* transcription/translation.

can be quantified by following the inhibition of methylation. The K_i value obtained from thiostrepton titrations (K_i = 2 ± 1 μM; data not shown) is in agreement with the value obtained in a nitrocellulose filter binding experiment, K_d = 1.3 ± 0.3 μM [27]. TSR methyltransferase is thus an intimate probe of intermolecular contacts in the L11BD. This assay was used to test other thiazole antibiotics. The effect of increasing L11BD concentration on A1067 methylation at fixed antibiotic concentration was measured (Figure 2C). Methylation was inhibited by thiostrepton (K_i = 3.9 μM), siomycin (K_i = 2.4 μM), and nosiheptide (K_i = 0.6 μM). No significant inhibition by micrococcin was detected at up to 10 μM antibiotic.

NMR Studies of a Stable L11BD-Thiostrepton Complex

The poor aqueous solubility of thiostrepton has until now impeded its structural analysis in the presence of RNA. We have developed a concentration protocol that relies on the affinity of thiostrepton for the L11BD in order to bring the complex into the millimolar concentration range for NMR studies. A stable bimolecular complex can be formed at 1 mM by 1000-fold concentration of a 1 μM solution of thiostrepton and L11BD. The abundance of methyl groups on thiostrepton allows the antibiotic to be directly observed in a one-dimensional (1D) NMR spectrum of the complex, as the 0–2 ppm region is generally unobstructed by RNA signals (Figure 3A). Other protons on the thiostrepton molecule do overlap with RNA signals, but, using two-dimensional (2D) NMR experiments (Figure 3B), most of the amide and side chain resonances could be assigned for the two macrocycles of thiostrepton (see Supplemental Table S1 at http://www.chembiol.com/cgi/content/full/10/8/769/DC1). Assignments were aided by both chemical shift data of thiostrepton in DMSO [28] and by observation of NOESY and TOCSY crosspeak patterns characteristic of the spin systems. Unassigned resonances were believed to be masked by the mass of RNA resonances between 4 and 8 ppm. The olefinic resonances on the dehydroalanine tail, DHA1 and DHA2 (Figure 1B), could not be detected, making it impossible to constrain this region of the molecule in subsequent modeling efforts. The NOESY spectrum of the complex (Figure 3B) was analyzed for thiostrepton intramolecular contacts, summarized schematically in Figure 3C. Inspection of the thiostrepton crystal structure [29] confirms that the interproton distance corresponding to each of the NOEs observed by NMR is less than 5 Å in the crystal structure, suggesting that thiostrepton does not undergo a large

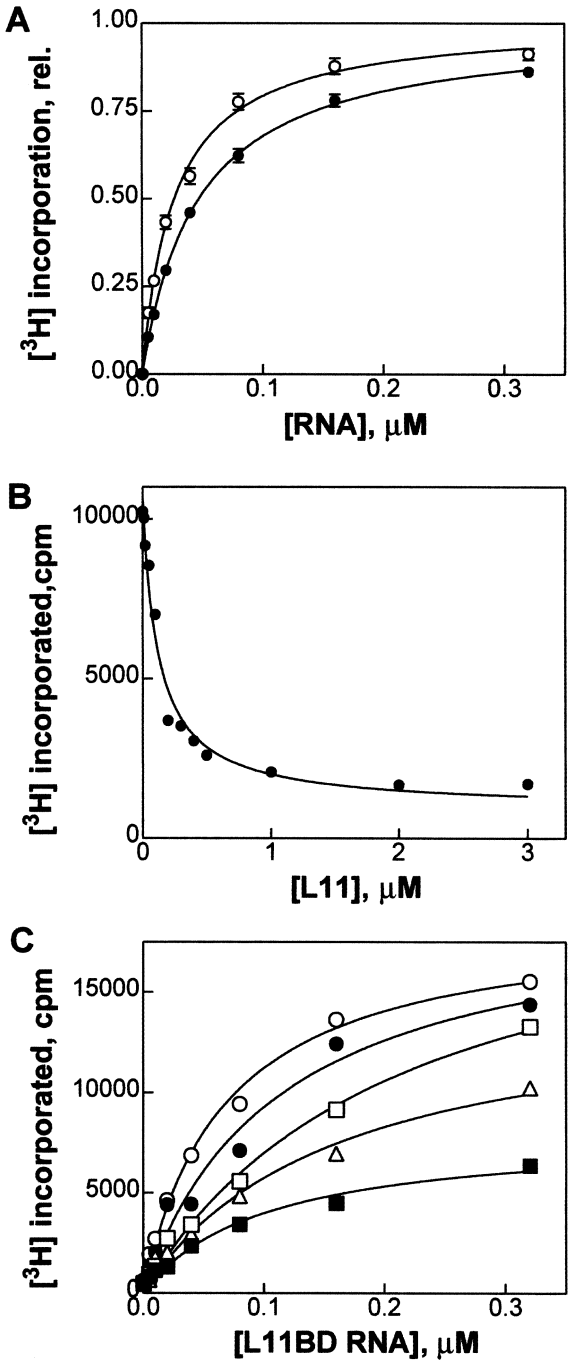

Figure 2. Methylation of L11BD RNA by TSR Methyltransferase

(A) Total ribosomal RNA (open circles) or a transcript corresponding to nucleotides 1051–1108 of 23S rRNA L11BD RNA (closed circles) was incubated with 8 pmol GST-TSR and 1 μCi [^{3}H]SAM for 15 min at 25°C. Methyl incorporation into RNA was quantified after TFA precipitation by scintillation counting. The graph shows average incorporation curves from 20 (total rRNA) and 15 (L11BD transcript) independent titrations. Half-maximal incorporation is reached at 30 (total rRNA) and 50 nM (L11BD RNA) respectively.

(B) Inhibition of L11BD methylation by ribosomal protein L11. Half-maximal inhibition is reached at 120 nM L11.

(C) Inhibition of L11BD methylation by thiazole antibiotics. TSR methyltransferase was titrated with L11BD RNA in the absence (open circles) and presence of thiazole antibiotics: 10 μM micrococcin (closed circles), 5 μM siomycin A (open triangles), 5 μM thiostrepton (open squares), 5 μM nosiheptide (closed squares).

conformational rearrangement on binding L11BD. However, close analysis of the intra- and intermolecular NOEs suggested some conformational flexibility, which was taken into account during subsequent calculations.

Specific Intermolecular Contacts

The large size of the L11BD construct and unfavorable dynamics made the RNA-specific NMR data unsuitable for sequence-specific assignment. Complete assignment of the thiostrepton resonances was not possible in the complex, due to resonance overlap between 4 and 8 ppm with the unresolved RNA signals. This made it impossible to distinguish between inter- and intramolecular NOEs involving the thiostrepton methyl resonances. To overcome this, a L11BD construct in which the A and C nucleotides were uniformly ^{13}C/^{15}N labeled was synthesized and complexed with thiostrepton. Using this partially labeled RNA in conjunction with ^{12}C/^{13}C half-filtered proton-proton NOESY experiments, it was possible to identify seven intermolecular NOEs. Although the RNA could not be assigned due to complexity of the spectra, ^{13}C chemical shift and proton dimension lineshape analysis allowed base-specific assignments to be made for the intermolecular NOEs [30]. Thus, three different AH2 protons and one AH8 had six intermolecular NOEs with the dehydrobutyrine (DHB)-containing macrocycle of thiostrepton, shown schematically in Figure 3C. One ambiguous NOE from the Hγ methyl protons of DHB to an H1′ of an A or a C nucleotide was also identified. Of particular interest was the fact that intermolecular NOEs were localized to one side of the DHB-containing macrocycle.

Thiazoles Share a Common Binding Mode

Using unlabeled L11BD RNA, the NMR analysis was repeated with siomycin, nosiheptide, and micrococcin. All formed stable 1:1 complexes with the L11BD construct, although the micrococcin complex was less stable over time (see Experimental Procedures). Not surprisingly, the siomycin complex NOESY spectrum was essentially identical to that of the thiostrepton complex (data not shown). The nosiheptide spectrum showed differences as compared to the thiostrepton complex, mostly attributable to differences in the second, indole-containing macrocycle (IND, Figure 1D). However, a remarkable similarity in both the intra and intermolecular NOEs involving the common DHB residue was observed (Figure 3D). The fact that these NOESY crosspeaks are practically superimposable strongly suggests similar binding modes for thiostrepton, siomycin, and nosiheptide. These same crosspeaks were not observed for the micrococcin complex. This indicates that the signals are either unobservable due to differences in relaxation properties or that micrococcin has a different L11BD binding mode than the other antibiotics.

Modeling of the L11BD-Thiostrepton Complex

A 3D model of the L11BD-thiostrepton complex was generated using the crystal coordinates of each component and rigid-body docking calculations [31]. The docking, performed with our rapid-docking program rDock (D. Morley et al., personal communication), was driven by the intermolecular NOE restraints. This NMR data

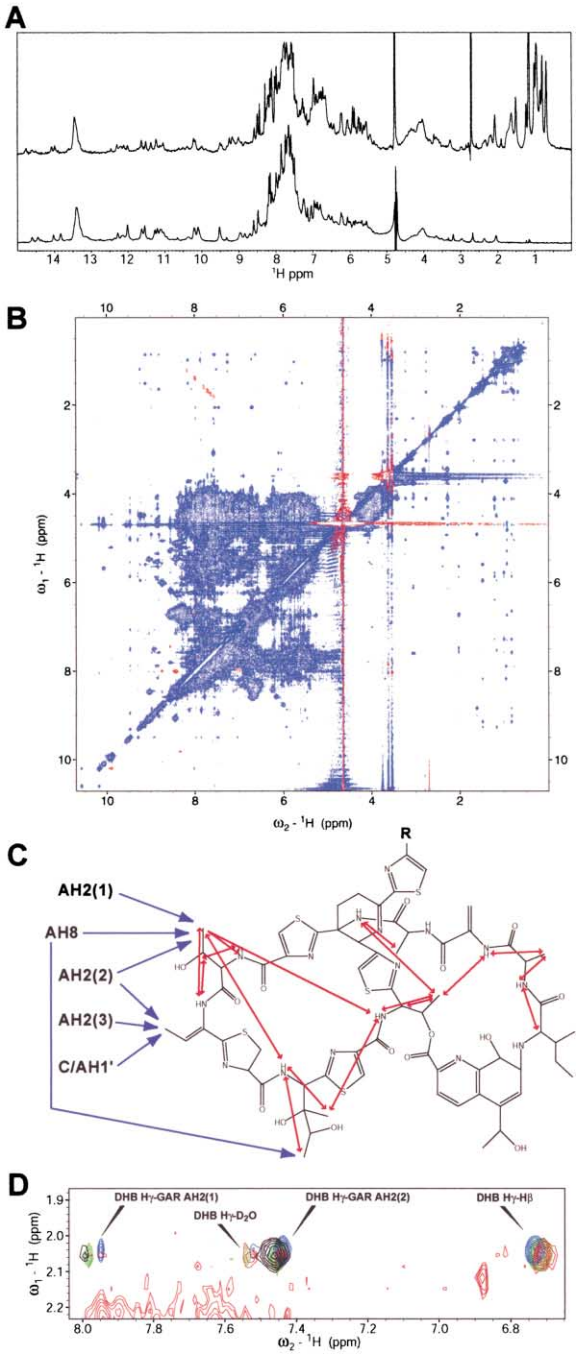

Figure 3. NMR Results for the L11BD-Thiostrepton Complex

(A) 1D NMR spectra for L11BD alone (bottom) and the L11BD-thiostrepton complex (top).

(B) 2D NOESY spectrum (250 ms mixing time) of the complex. Inter- and intramolecular NOEs involving the thiostrepton methyl resonances are visible as resolved blue crosspeaks. Negative signal artifacts are in red.

(C) Schematic representation of observed intramolecular NOEs (red twin-headed arrows) and intermolecular L11BD-thiostrepton NOEs (blue single-headed arrows). The dehydroalanine tail (R) is not shown.

(D) Superposition of NOESY spectra showing the region containing NOEs between the DHB methyl (Hγ) protons and the aromatic region of the spectrum. NOESY crosspeaks for thiostrepton (blue), siomycin (green), and nosiheptide (red) complexes are shown with ^{12}C/^{13}C half-filtered NOESY peaks (intermolecular NOEs) for the A/C-^{15}N/^{13}C-labeled L11BD-thiostrepton complex (black). Four NOEs are labeled: the intramolecular Hγ-Hβ NOE of the DHB residue (right), the L11BD AH2(2)-DHB Hγ intermolecular NOE (center-right), an unassigned NOE involving a nonexchangeable L11BD or antibiotic proton (center-left, labeled "D_2O"), and the second L11BD AH2(1)-DHB Hγ intermolecular NOE (left).

has shown that the H2 protons of three adenosine nucleotides give NOEs to thiostrepton (Figure 3C). Since we lacked sequence specific assignments for the L11BD resonances, separate calculations were run for each possible set of assignments. Based upon published biochemical data, it was assumed that the three adenosine residues contacting thiostrepton could be drawn from the seven which show chemical modification footprints in the presence of thiazole antibiotics, positions 1067, 1069, 1070, 1073, 1095, 1096, and 1098 [8, 16]. This assumption gave rise to 210 potential assignment sets corresponding to each possible combination of three adenosine H2 assignments. In a first stage, only these three NOEs were considered. Each of the possible assignment sets was run 200 times, and the resulting structures were filtered based on the NOE violations and the rDock scoring function (see Experimental Procedures). One set of AH2 assignments yielded converged docked structures with the best agreement with NOE data as well as the best overall score. A similar process was implemented during a second stage of calculations, incorporating the three AH2 assignments preferred during the first stage but testing the possible assignment sets for the remaining intermolecular NOES. This process generated a self-consistent model for thiostrepton binding to L11BD (Figure 4). The lowest energy set of structures was obtained with the following assignments (cf. Figure 3C): AH2(1) = A1095, AH2(2) = A1067, AH2(3) = A1096, AH8 = A1067, and C/AH1′ = A1096. This represents the part of the molecule with the densest cluster of AH2 resonances, giving rise to the set of three NOEs observed in the complex. The protocol assumes that the L11BD RNA fold in the presence of thiostrepton is similar to that observed in the cocrystal with L11.

The model (Figure 4) reveals stacking of the quinaldic acid (QA) residue on A1067 and stacking of the thiazole moiety (THZ), common to all four antibiotics, directly over A1095. The position of the QA-containing macrocycle is consistent with the inhibition of methylation at the N1 and 2′O positions on A1067 (both highlighted as spheres in Figure 4). The DHB-containing macrocycle, which shows NOEs to L11BD, sits near the minor groove face of the two critical A residues, accounting for two of the NOEs to AH2 resonances.

Effect of Thiazole Antibiotics on GTP Hydrolysis by EF-G

The effects of the four thiazoles on EF-G-dependent GTP hydrolysis were measured under multiple-turnover conditions on nonprogrammed, vacant ribosomes at 20°C. In the presence of catalytic amounts of EF-G (3- to 5-fold excess of ribosomes), γ-[^{32}P]GTP hydrolysis was suppressed by thiostrepton, nosiheptide, and siomycin and strongly increased by micrococcin during 10

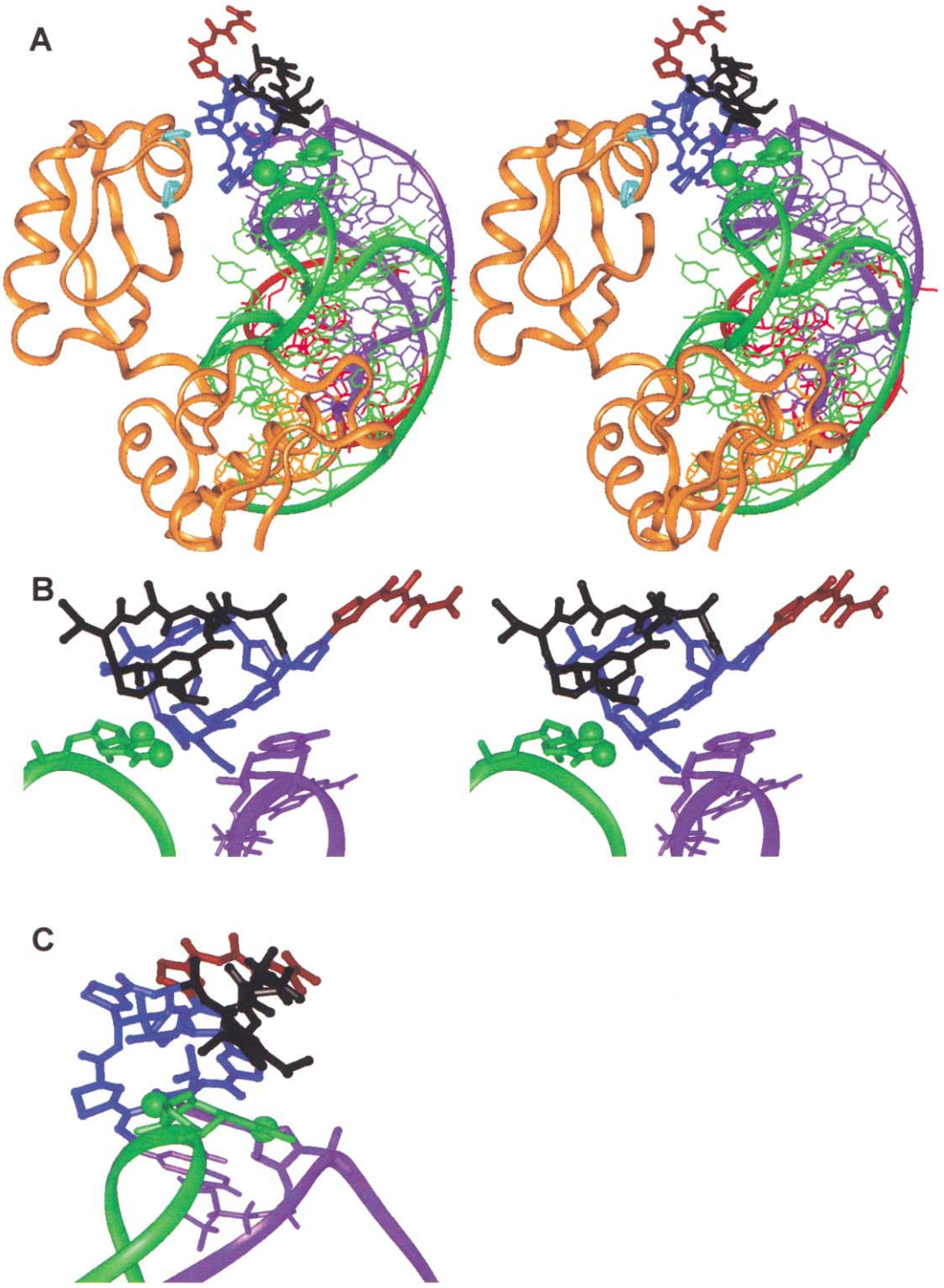

Figure 4. L11BD-Thiostrepton Binding Model

(A) The crystal structure of L11 bound to L11BD [24] is overlaid onto the L11BD coordinates. A1067 and A1095 on L11BD are rendered in liquorice. Protein ribbon is highlighted in orange, common DHB containing macrocycle in blue, QA containing macrocycle in black, and RNA color coding follows the convention of [24]. The 2′OH and N1 of A1067 are rendered as spheres. Proline positions in the N terminus of L11 (P23 and P26) which, when mutated, confer resistance to micrococcin and thiostrepton are highlighted in light blue.

(B) Close-up stereo view of thiostrepton binding site.

(C) 90 degree rotation of view presented in (B).

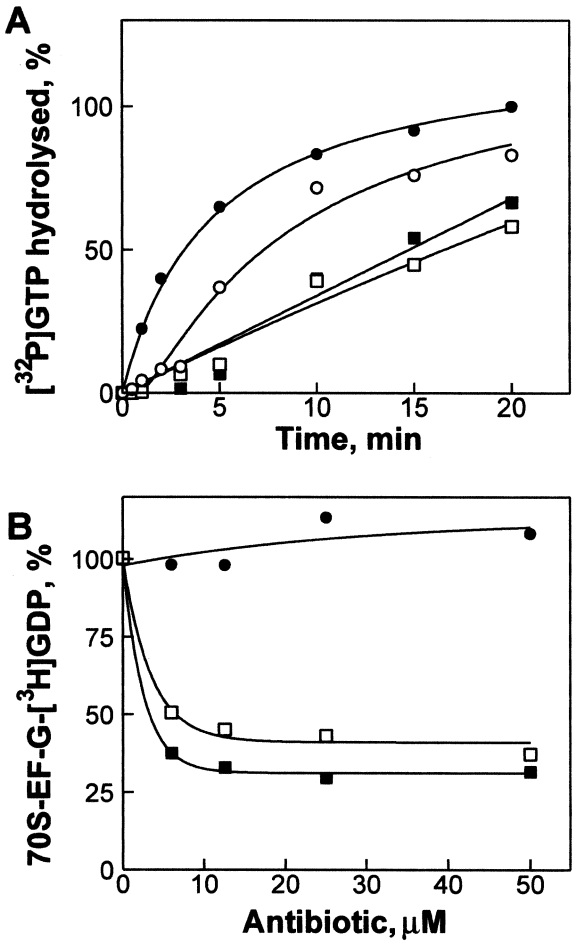

Figure 5. Effect of Thiazole Antibiotics on Uncoupled EF-G-Dependent GTP Hydrolysis and 70S Ribosome-EF-G-GDP Complex Formation

(A) Effect of thiazole antibiotics on uncoupled EF-G-dependent hydrolysis of γ-[^{32}P]GTP on the ribosome. Reactions were performed under the multiple-turnover conditions in 2% DMSO in the absence (open circles) and presence of micrococcin (closed circles), thiostrepton (open squares), or nosiheptide (closed squares) at 20°C. Background counts due to GTP hydrolysis in the absence of either ribosomes or EF-G have been subtracted.

(B) Effect of thiazole antibiotics on the 70S ribosome-EF-G-[^{3}H]GDP complex formation. Reaction mixtures were incubated at 4°C for 20 min in the presence of 2% DMSO, 1 mM fusidic acid, and micrococcin (closed circles), thiostrepton (open squares), or nosiheptide (closed squares). Analysis by filtration through the 0.45 μm membrane. Background counts of radioactivity bound to ribosome in the absence of EF-G were subtracted to give the values shown.

min incubations (Figure 5A). After 45 min, almost all of the GTP present was hydrolyzed (data not shown). In the presence of 2- to 3-fold excess of EF-G over ribosomes, the effect of thiostrepton, nosiheptide, and siomycin was insignificant; after 3 min, almost all of the GTP initially present was hydrolyzed (data not shown). In the presence of micrococcin, GTP hydrolysis was complete in less than 30 s (data not shown). Single-turnover GTP hydrolysis could not be resolved using this technique and time range. These findings are in agreement with results published for thiostrepton [14]. Rodnina and coworkers demonstrated that thiostrepton inhibited the turnover of EF-G on the ribosome but not its GTPase activity. Data presented here demonstrate that in addition to thiostrepton, nosiheptide and siomycin have similar effects on GTP hydrolysis, which differ from the effects produced by micrococcin. Thus, in the presence of thiazole antibiotics, only the turnover of EF-G on the ribosome is affected (decreased or increased), whereas the full extent of GTP hydrolysis takes place.

Effect of Thiazoles on EF-G-GDP Binding to the Ribosome

In the absence of antibiotics, EF-G binds to the ribosome, hydrolyzes GTP, and EF-G-GDP dissociates from the ribosome. A complex between EF-G-GDP and vacant ribosomes can be stabilized by fusidic acid (FA). FA binds to EF-G on the ribosome and inhibits the structural transition of EF-G at the last stage before dissociation of the factor from the ribosome. A single round of GTP hydrolysis takes place, but EF-G-GDP cannot dissociate from the ribosome [10, 32]. We examined the effect of thiazoles on the formation of the FA-stabilized EF-G-GDP-ribosome complex in the presence of [^{3}H]GTP by filtration of the complex through a 0.45 μm membrane. The amount of EF-G-GDP bound to the ribosome was significantly reduced in the presence of thiostrepton, nosiheptide (Figure 5B), or siomycin (data not shown). Micrococcin behaves differently. We were unable to detect any effect of micrococcin on the FA-stabilized binding of EF-G-GDP to the ribosome at up to 50 μM antibiotic.

Discussion

The Mode of Action of Thiazole Antibiotics

Early studies on the mode of action of thiazole antibiotics produced conflicting evidence, suggesting interference with either the ribosomal A site, translational factors EF-G, EF-Tu, and IF-2, or stringent factor [14, 15, 22, 33]. We examined the mode of action and binding of four thiazole antibiotics. All were confirmed to be selective inhibitors of bacterial translation (Table 1). We have shown by NMR that nosiheptide interacts directly with L11BD and have found that nosiheptide, thiostrepton, and siomycin have similar L11BD binding modes. The effects of nosiheptide and siomycin on TSR methyltransferase-catalyzed modification of A1067 (Figure 2), EF-G-dependent GTP hydrolysis, and FA-stabilized EF-G-GDP binding to the ribosome are similar to those of thiostrepton. In contrast, micrococcin accelerates GTP hydrolysis and does not show any significant effect on methylation and EF-G-GDP binding. These observations reinforce earlier reports that micrococcin and thiostrepton have differential effects on the ribosome, suggested by opposite effects on EF-G-dependent GTP hydrolysis [12, 22] and protection from chemical modification by DMS [17]. In addition, these data place nosiheptide in the same category as thiostrepton in its mode of interaction, in agreement with our NMR results.

Inspection of the chemical structures of the thiazole antibiotics studied reveals a conserved region surrounding the DHB residue (Figure 1). This region ac-

counts for six of the seven intermolecular NOEs identified in the thiostrepton-L11BD complex. The importance of this conserved region is underscored by our finding that GE2270A, another thiazole antibiotic that does not contain the DHB region [34], does not bind L11BD (data not shown).

Our results support the idea that the binding of the thiazole antibiotics can favor a particular structure and perturb conformational equilibria. We have demonstrated that binding of thiostrepton, nosiheptide, and siomycin to L11BD results in a ribosome conformation that significantly retards the turnover of EF-G (but not GTP hydrolysis) on ribosomes (Figure 5A). Concurrently, the stabilizing effect of FA on the EF-G-GDP-ribosomal complex is reduced (Figure 5B). This suggests that in the presence of thiostrepton, siomycin, and nosiheptide, EF-G can bind to the ribosome and hydrolyze GTP, but the structure of ribosome-EF-G-GDP differs from the one that is fixed by FA. This observation is consistent with previous results [14] demonstrating that thiostrepton decreased the turnover of EF-G and interfered with subsequent steps—release of inorganic phosphate from EF-G after GTP hydrolysis and dissociation of the factor from the ribosome.

Literature data on the mode of action of micrococcin is limited [12, 15, 22 and references within]. Micrococcin has been reported to increase GTP hydrolysis and decrease stabilization of EF-G on the ribosome by fusidic acid. It was proposed that antibiotic destabilized the EF-G-ribosomal complex after GTP hydrolysis and accelerated the dissociation of the factor from the ribosome. Our data demonstrate that micrococcin accelerates GTP hydrolysis and does not interfere with the stabilizing effect of fusidic acid (Figure 5). It is the acceleration of GTP hydrolysis that leads to a more rapid dissociation of EF-G from the ribosome. The conformation of the EF-G-ribosomal complex after GTP hydrolysis, before factor leaves the ribosome, is similar to one which can be frozen by fusidic acid. This conclusion differs from that of some earlier reports, probably in part due to wide variations in experimental conditions such as temperature, ionic composition, EF-G, ribosome and antibiotic concentration, and techniques used (see [14, 15, 22] for comparison). Moreover, EF-G-ribosomal complexes containing thiazoles are likely to be too labile to be detected by nonequilibrium methods (see [14, 15] for comparison). The data presented here demonstrate that micrococcin blocks translation in a different manner from that of thiostrepton, siomycin, and nosiheptide. We suggest that whereas thiostrepton, siomycin, and nosiheptide decrease the overall turnover of EF-G, micrococcin increases it.

The L11BD-Thiostrepton Binding Model

In building the L11BD-thiostrepton model, we have assumed that both components of the system are held rigidly to the conformations observed in their corresponding X-ray structures. This assumption does not allow for the induced fit of one or both components, which is almost certainly taking place, or the displacement of bound ions or water molecules [24, 25]. Despite these limitations, the model provides considerable insight into the current understanding of the binding mode of thiostrepton to this region of RNA.

The binding mode of micrococcin remains unknown. Although structural differences between the thiostrepton and micrococcin complexes cannot be ruled out, the chemical and enzymatic footprinting results for each complex can be rationalized by the thiostrepton-L11BD model. While all four thiazoles contain a common DHB macrocycle, highlighted in blue in Figure 4, micrococcin lacks the second QA- or IND-containing macrocycle. The model situates the DHB-containing macrocycle over A1095, accounting for the protection of this residue from chemical modification by thiostrepton and micrococcin. The QA-containing macrocycle of thiostrepton is located over A1067. We propose that this second macrocycle is responsible for inhibiting access of both TSR methyltransferase (Figure 2C) and DMS to A1067. The absence of this macrocycle in micrococcin would leave the A1067 2′OH and N1 positions more accessible to modification. We also propose that the IND moiety substitutes for the QA residue in nosiheptide and would be positioned to hinder access to A1067, thus explaining the "thiostrepton-like" behavior of nosiheptide. Fluorescence data (not shown) support the proposed model. While fluorescence associated with thiostrepton is quenched in aqueous solution, on binding to L11BD thiostrepton fluorescence is observed, and the excitation and emission maxima are blue shifted. These shifts are consistent with the stacking of this residue on A1067 as postulated in Figure 4.

The model in Figure 4 was generated using NMR data collected in the absence of L11. Inclusion of the protein's X-ray coordinates provides a rationale for published data regarding L11-thiazole antibiotic interactions. Thiostrepton binding stabilizes the L11/L11BD complex, and the presence of L11 increases the affinity of thiostrepton for L11BD [19]. Resistance mutations on the N terminus of L11 provide evidence for direct thiazole-protein interactions. According to the model, prolines 23 and 26 (highlighted in cyan in Figure 4A), which when mutated are associated with micrococcin and thiostrepton resistance [18, 35], are proximal to the DHB-containing macrocycle. It is possible that this macrocycle plays a role in the stabilization of the L11/L11BD complex through RNA *and* protein contacts. Many of the L11 thiazole resistance mutants are more susceptible to thiostrepton than to micrococcin [18, 35]. This could be explained by additional stacking interactions at A1067 by the QA macrocycle in thiostrepton, which would stabilize the complex in a protein-independent manner.

The differential effects of thiostrepton and micrococcin on EF-G-dependent GTP hydrolysis and the formation of the ribosome-EF-G-GDP complex are also consistent with our model. Chemical modification by DMS [10], direct hydroxyl radical probing with Fe(II)-tethered EF-G [36], and crosslinking [9] have demonstrated the proximity of EF-G to the A1067 loop of 23S rRNA. Cryo-electron microscopy (cryo-em) maps have placed domain V of EF-G within 4 Å of the A1067 loop [37]. Therefore, if the QA macrocycle is situated above A1067, one predicts that EF-G interaction with L11BD would be hindered by thiostrepton but not by micrococcin, as

we have observed. Moreover, another cryo-em study showed significant changes in the placement of EF-G ribosomal complexes with thiostrepton present, both pre- and post-translocation [38]. Based upon our model, we would suggest that thiostrepton (and nosiheptide and siomycin) induces these effects and resulting effects on EF-G-dependent GTP hydrolysis, at least partly via a steric block of EF-G contacts on ribosomal RNA. Micrococcin, on the other hand, can be expected to hinder translocation by disrupting the timing and coupling of associated reactions.

Enzymatic Methylation of A1067 as an Assay for Binding to L11BD rRNA

Methylation of A1067 by TSR methyltransferase is inhibited by binding of agents that interact with L11BD at A1067, including L11 and thiostrepton. This result implies that the resistance methylation occurs before L11 joins the ribosome during biogenesis [33]. Inhibition of A1067 methylation can be used to quantify interactions at this site. The affinities for L11 and thiostrepton obtained from this assay are in good accord with the affinities measured in direct binding experiments, e.g., nitrocellulose filter binding. Siomycin and nosiheptide show similar binding affinities as thiostrepton. We have shown that the methyltransferase reaction can be used as a probe for novel compounds binding to L11BD [39, 48], suitable for the high-throughput screening of chemical libraries. This assay is a valuable tool for the discovery of novel antiinfectives targeting L11BD, a validated but so far clinically unexploited target.

Significance

Micrococcin and thiostrepton contain common structural features and act on the same target, but with differing effects on ribosomal function. We propose an explanation for this apparent paradox, based upon a structural model for the interaction of thiostrepton with the L11BD. Although the model ignores possible conformational changes, the global features are strongly supported by all of the findings reported here and by many reported previously regarding thiazole-L11BD interactions.

The QA heterocycle is the major structural difference between thiostrepton and micrococcin. Our model places the QA heterocycle directly above the critical A1067 residue. From this position, the QA will interfere with EF-G binding and turnover. Therefore, one would predict that thiostrepton would interfere with these functions, as has been observed in this study and elsewhere, while micrococcin will have different effects. We showed that A1067, predicted to be involved in a stacking interaction with the QA heterocycle, is protected from modification by TSR methyltransferase by the presence of thiostrepton and not by micrococcin.

Another prediction of the model is that related thiazole compounds will produce similar biochemical footprints and functional effects to those produced by thiostrepton and micrococcin, according to the presence or absence of an aromatic group in a position to substitute for the A1067 stacking of the QA moiety. Indeed, we have shown that nosiheptide, which contains such a potential stacking group, binds to the L11BD and produces effects on EF-G-dependent GTP hydrolysis, EF-G binding, and TSR methyltransferase activity which are identical to those of thiostrepton. Futhermore, intermolecular NOEs appear in the NOESY spectrum of the nosiheptide complex with L11BD, which demonstrates that the binding mode of nosiheptide to L11BD resembles that of thiostrepton, as predicted.

Overall, these results point toward a novel molecular mechanism for antibiotic inhibition of translation and potential strategies for designing new antibiotic compounds.

Experimental Procedures

Materials and Buffers

Micrococcin, siomycin A, and nosiheptide were kindly provided by H.G. Floss, University of Washington. GE2270A was a gift from S. Donadio, Biosearch Italia. Radiochemicals S-adenosyl-L- methyl-[^{3}H]methionine ([^{3}H]SAM), γ-[^{32}P]GTP, and 8-[^{3}H]GTP were from Amersham Biosciences. PEC plates were from Macherey-Nagel. 96-well glass fiber (MultiScreen FB) and 0.45 μm cellulose ester (MultiScreen HA) filter plates were from Millipore. All chemicals were from Sigma. Antibiotics were dissolved in dimethylsulfoxide (DMSO). Buffers: (A), 50 mM Tris-HCl (pH 7.5), 70 mM NH_4Cl, 30 mM KCl, 7 mM $MgCl_2$, 2 mM DTT; (B), 25 mM HEPES-KOH (pH 7.5), 25 mM NH_4Cl, 5 mM $MgCl_2$, 5 mM DTT; (C), 10 mM potassium phosphate (pH 6.2), 100 mM KCl, 5 mM $MgCl_2$.

Experimental Procedures

Salt-washed 70S ribosomes from *E. coli* MRE 600 were purified as described [40, 41]. Wild-type EF-G and C-terminal $(His)_6$-tag EF-G (a kind gift from M. Rodnina and A. Savelsbergh, University Witten/Herdecke) were expressed in *E. coli* and purified as described [42, 43].

In Vitro Translation Assay

The coupled transcription/translation was performed as described [44] using *E. coli* S30 extract with the pBestLuc plasmid (Promega) as template in the presence of 2% DMSO. Translation reactions (10 μl) were incubated for 60 min at 37°C and quantified by measuring the luminescence in a Victor II plate reader (Perkin-Elmer) after addition of 50 μl luciferase reagent (Promega). Inhibition of translation by the thiazoles was confirmed in an uncoupled translation system using MS2 bacteriophage RNA (Roche) as template and measuring the incorporation of [^{3}H]methionine (data not shown). Eukaryotic translation was measured in rabbit reticulocyte lysate (Promega) with an mRNA coding for firefly luciferase [45].

L11BD RNA

A 60 nucleotide RNA construct containing 1051–1108 of the *Thermatoga maritima* 23S rRNA sequence was used in all experiments (Figure 1A). An additional G·U base pair was added to extend the terminal stem to improve the transcription yield. Milligram quantities were prepared by synthetic DNA template-driven T7 RNA polymerase transcription. T7 RNA polymerase was expressed and purified in-house, and transcription conditions and acrylamide gel purification were as previously reported [46]. Typically, a 20 ml transcription reaction produced 10–15 mg of purified RNA.

Expression Cloning of TSR Methyltransferase

The *Streptomyces azureus tsr* gene from the plasmid pIJ2581 (provided by M. Bibb, John Innes Foundation, Norwich) [47] was cloned by PCR using the primers GGTGGTGGATCCATGACTGAGTTGGA CACC and GTGGTGGAATTCTTATTACGGTTGGCCGC. The PCR product was ligated with the correspondingly linearized vector pGEX-2T to yield an expression construct (pGEX-TSR) expressing a gluta-

thion-S-transferase fusion protein (GST-TSR). Identity was confirmed by sequencing.

The protein was overexpressed in *E. coli* JM109 cells transformed with pGEX-TSR using 0.1 mM IPTG for induction of a mid-log culture of transformed cells. Cells were grown for 3 hr after induction, harvested, and then lysed by sonication. GST-TSR was purified by affinity chromatography using Glutathion Sepharose 4B (Amersham Biosciences). Electrophoretically pure TSR could be obtained by thrombin cleavage of the fusion protein. The fusion protein and the native TSR methyltransferase showed similar enzymatic activity (data not shown). Methyltransferase assays were therefore performed using the GST-TSR fusion protein.

TSR Methyltransferase Assay

TSR methyltransferase activity was investigated using *E. coli* rRNA and the L11BD construct. RNA (0–0.32 μM) was incubated in buffer B, 1% DMSO. When testing thiazole antibiotics, the DMSO concentration was increased to 10% to improve solubility. The reaction (100 μl) was started by adding 8 pmol TSR methyltransferase and 1 μCi [^{3}H]SAM. The reaction was incubated for 15 min at 25°C and stopped by 1 volume of 2% TFA. The TFA precipitate was filtered through a 96-well glass fiber filter plate. The filters were washed with 2 volumes of 2% TFA and dried. Scintillation cocktail (50 μl) (Optiszint, PerkinElmer) was added to each well, and [^{3}H]-radioactivity was determined in a Trilux scintillation counter (PerkinElmer).

K_m values were calculated using the equation $y = B_{max}*[RNA]/(K_m + [RNA])$, where B_{max} is incorporation at RNA saturation, [RNA] is concentration of RNA, and K_m is the Michaelis constant. The K_i values for the thiazole antibiotics were determined using the equation $K_i = [I]/((K_m(I)/K_m) - 1)$, where [I] is concentration of the inhibitory compound, and K_m and $K_m(I)$ are the Michaelis constants in the presence and absence of inhibitor.

GTPase Activity

Uncoupled GTP hydrolysis was performed essentially as described [14, 22]. Assays were carried out in buffer A in 2% DMSO with or without 50 μM antibiotics. γ-[^{32}P]GTP hydrolysis was measured either by thin-layer chromatography (TLC) or by adsorption onto activated charcoal. EF-G (0.04 μM) was preincubated with 70S ribosomes (0.25 μM) for 15 min at 37°C and mixed with 5–20 μM γ-[^{32}P]GTP. Samples were quenched either with formic acid or $HClO_4$. Charcoal was removed and [^{32}P]phosphate was either counted on a Trilux radioactivity counter (PerkinElmer) in 96-well plates or quantified using a Phosphorimager. When quantification was by TLC, the ratio of [^{32}P]phosphate to γ-[^{32}P]GTP was determined using a Phosphoimager

EF-G-GTP Binding to Ribosomes

Assays were carried out in buffer A containing 1 mM fusidic acid (FA), 15 mM $MgCl_2$, and 2% DMSO. EF-G (2 μM) was incubated with 8-[^{3}H]GTP at 37°C for 5 min, mixed with an equal volume of 70S ribosomes (0.5 μM), incubated at 4°C for 20 min, and filtered through 96-well filter plates (MultiScreen HA; 0.45 μm). Filters were washed four times with buffer A with 0.2 mM FA and dried. Radioactivity was estimated by liquid-scintillation spectrometry on a Trilux scintillation counter (PerkinElmer) in 96-well plates with 50 μl scintillation cocktail (Optiszint, PerkinElmer).

^{13}C/^{15}N AMP,CMP Incorporation

Uniformly ^{15}N/^{13}C-labeled adenosine and cytosine monophosphates (Martek) were phosphorylated to triphosphates in a one-pot reaction and purified on a boronate column (BioRad) as previously described [30]. These were combined with unlabeled GTP and UTP (Sigma) and used at 8 mM each NTP in a 10 ml transcription reaction as described above, yielding 6 mg of purified A,C-labeled RNA.

RNA-Thiazole Antibiotic Complex Formation

A stable 1:1 complex of RNA and thiazole antibiotic was formed at low micromolar concentrations by diluting a 1 mM aqueous stock solution of RNA and a 10 mg/ml solution of thiazole antibiotic in DMSO to 1 μM and 2 μM, respectively, in 250 ml of buffer C. After incubation with stirring for 4 to 16 hr at 4°C, the solution was concentrated to 250 μl by centrifugation using 5 kDa molecular weight cutoff Biomax Ultrafree-CL units (Millipore). The relative amount of each component in the complex was determined to be 1:1 by integration of RNA and antibiotic-specific regions of the 1D NMR spectrum in D_2O (data not shown). Thiostrepton, siomycin, and nosiheptide complexes prepared in this way were stable for several weeks at temperatures between 4°C (storage) and 30°C (NMR experiments). The RNA-micrococcin complex was less stable; precipitation of the antibiotic was visible after 1 day at 30°C. As a control, the complex formation protocol was attempted with thiostrepton and a 78 nucleotide construct containing nucleotides 2107–2182 of *E. coli* 23S rRNA (the L1 protein binding site). After the concentration step, no thiostrepton could be detected by NMR in the retentate (data not shown).

NMR

NMR experiments were carried out on Bruker DRX500 and AV600 spectrometers equipped with four-channel ^{1}H/^{31}P/^{13}C/^{15}N gradient probes. Standard experimental conditions were 0.5 to 1 mM RNA (free or complexed with antibiotic) in buffer C at 30°C. Ten percent D_2O was added for final sample volumes of 280 μl in low-volume NMR tubes (Shigemi). NOESY and TOCSY experiments were recorded in both H_2O and D_2O on the unlabeled complex. ^{12}C/^{13}C-half filtered NOESY and ^{1}H-^{13}C HSQC experiments were used to identify intermolecular NOEs in the ^{13}C/^{15}N A,C-labeled RNA-antibiotic complex ([30] and references therein).

Model for Thiostrepton Interaction with L11BD

Docking calculations were run on a Linux cluster using a Condor distribution system (http://www.cs.wisc.edu/condor/). Coordinates from the X-ray structures of L11BD (PDB ID code 1MMS) and thiostrepton (PDB ID code 1E9W) were used in the calculations. The docked structures were filtered based on the NOE violations and the rDock scoring function, which includes aromatic, polar, and van der Waals terms. This allows for the benefit of the rDock empirical scoring function to partly compensate for the sparseness of the NOE dataset. Both components were held rigid during docking. The model should be viewed as an indication of binding mode and some aspects of the interaction as suggested by NMR and biochemical data, rather than a detailed description of the 3D structure of the complex. The details of the modeling protocol will be described elsewhere (R.K. et al., unpublished data).

Acknowledgments

We thank Szilveszter Juhos and Dave Morley for assistance with the use of rDock, Ben Davis for helpful discussions, Jonathan Karn and David Knowles for support and advice on this project, and Venki Ramakrishnan and Wolfgang Wintermeyer for helpful comments on the manuscript. This work was supported by a grant from the European Commission, contract no. QLK2-CT-2002-00892.

Received: May 2, 2003
Revised: June 13, 2003
Accepted: June 27, 2003
Published: August 22, 2003

References

1. Wimberly, B.T., Brodersen, D.E., Clemons, W.M., Jr., Morgan-Warren, R.J., Carter, A.P., Vonrhein, C., Hartsch, T., and Ramakrishnan, V. (2000). Structure of the 30S ribosomal subunit. Nature *407*, 327–339.
2. Ban, N., Nissen, P., Hansen, J., Moore, P.B., and Steitz, T.A. (2000). The complete atomic structure of the large ribosomal subunit at 2.4 Å resolution. Science *289*, 905–920.
3. Harms, J., Schluenzen, F., Zarivach, R., Bashan, A., Gat, S., Agmon, I., Bartels, H., Franceschi, F., and Yonath, A. (2001). High resolution structure of the large ribosomal subunit from a mesophilic eubacterium. Cell *107*, 679–688.
4. Yusupov, M.M., Yusupova, G.Z., Baucom, A., Lieberman, K., Earnest, T.N., Cate, J.H., and Noller, H.F. (2001). Crystal structure of the ribosome at 5.5 Å resolution. Science *292*, 883–896.
5. Knowles, D.J.C., Foloppe, N., Matassova, N.B., and Murchie, A.I.H. (2002). The bacterial ribosome, a promising focus for structure-based drug design. Curr. Opin. Pharmacol. *2*, 501–506.

6. Ramakrishnan, V. (2002). Ribosome structure and the mechanism of translation. Cell *108*, 557–572.
7. Schmidt, F.J., Thompson, J., Lee, K., Dijk, J., and Cundliffe, E. (1981). The binding site for ribosomal protein L11 within 23 S ribosomal RNA of Escherichia coli. J. Biol. Chem. *256*, 12301–12305.
8. Egebjerg, J., Douthwaite, S.R., Liljas, A., and Garrett, R.A. (1990). Characterization of the binding sites of protein L11 and the L10.(L12)4 pentameric complex in the GTPase domain of 23 S ribosomal RNA from Escherichia coli. J. Mol. Biol. *213*, 275–288.
9. Sköld, S.E. (1983). Chemical crosslinking of elongation factor G to the 23S RNA in 70S ribosomes from Escherichia coli. Nucleic Acids Res. *11*, 4923–4932.
10. Moazed, D., Robertson, J.M., and Noller, H.F. (1988). Interaction of elongation factors EF-G and EF-Tu with a conserved loop in 23S RNA. Nature *334*, 362–364.
11. Wintermeyer, W., and Rodnina, M.V. (2000). Translational elongation factor G: a GTP-driven motor of the ribosome. Essays Biochem. *35*, 117–129.
12. Gale, E.F., Cundliffe, E., Reynolds, P.E., Richmond, M.H., and Waring, M. (1981). The Molecular Basis of Antibiotic Action. (London: Wiley), pp. 402–457.
13. Thompson, J., Schmidt, F., and Cundliffe, E. (1982). Site of action of a ribosomal RNA methyltransferase conferring resistance to thiostrepton. J. Biol. Chem. *257*, 7915–7917.
14. Rodnina, M.V., Savelsbergh, A., Matassova, N.B., Katunin, V.I., Semenkov, Y.P., and Wintermeyer, W. (1999). Thiostrepton inhibits the turnover but not the GTPase of elongation factor G on the ribosome. Proc. Natl. Acad. Sci. USA *96*, 9586–9590.
15. Cameron, D.M., Thompson, J., March, P.E., and Dahlberg, A.E. (2002). Initiation factor IF2, thiostrepton and micrococcin prevent the binding of elongation factor G to the Escherichia coli ribosome. J. Mol. Biol. *319*, 27–35.
16. Rosendahl, G., and Douthwaite, S. (1994). The antibiotics micrococcin and thiostrepton interact directly with 23S rRNA nucleotides 1067A and 1095A. Nucleic Acids Res. *22*, 357–363.
17. Egebjerg, J., Douthwaite, S., and Garrett, R.A. (1989). Antibiotic interactions at the GTPase-associated centre within Escherichia coli 23S rRNA. EMBO J. *8*, 607–611.
18. Porse, B.T., Leviev, I., Mankin, A.S., and Garrett, R.A. (1998). The antibiotic thiostrepton inhibits a functional transition within protein L11 at the ribosomal GTPase centre. J. Mol. Biol. *276*, 391–404.
19. Xing, Y., and Draper, D.E. (1996). Cooperative interactions of RNA and thiostrepton antibiotic with two domains of ribosomal protein L11. Biochemistry *35*, 1581–1588.
20. Cundliffe, E., and Thompson, J. (1979). Ribose methylation and resistance to thiostrepton. Nature *278*, 859–861.
21. Spedding, G., and Cundliffe, E. (1984). Identification of the altered ribosomal component responsible for resistance to micrococcin in mutants of Bacillus megaterium. Eur. J. Biochem. *140*, 453–459.
22. Cundliffe, E., and Thompson, J. (1981). Concerning the mode of action of micrococcin upon bacterial protein synthesis. Eur. J. Biochem. *118*, 47–52.
23. Thompson, J., and Cundliffe, E. (1991). The binding of thiostrepton to 23S ribosomal RNA. Biochimie *73*, 1131–1135.
24. Wimberly, B.T., Guymon, R., McCutcheon, J.P., White, S.W., and Ramakrishnan, V. (1999). A detailed view of a ribosomal active site: the structure of the L11-RNA complex. Cell *4*, 491–502.
25. Conn, G.L., Draper, D.E., Lattman, E.E., and Gittis, A.G. (1999). Crystal structure of a conserved ribosomal protein-RNA complex. Science *284*, 1171–1174.
26. Bechthold, A., and Floss, H.G. (1994). Overexpression of the thiostrepton-resistance gene from Streptomyces azureus in Escherichia coli and characterization of recognition sites of the 23S rRNA A1067 2′-methyltransferase in the guanosine triphosphatase center of 23S ribosomal RNA. Eur. J. Biochem. *224*, 431–437.
27. Ryan, P.C., Lu, M., and Draper, D.E. (1991). Recognition of the highly conserved GTPase center of 23 S ribosomal RNA by ribosomal protein L11 and the antibiotic thiostrepton. J. Mol. Biol. *221*, 1257–1268.
28. Mocek, U., Beale, J.M., and Floss, H.G. (1989). Reexamination of the ^{1}H and ^{13}C NMR spectral assignments of thiostrepton. J. Antibiot. (Tokyo) *11*, 1649–1652.
29. Bond, C.S., Shaw, M.P., Alphey, M.S., and Hunter, W.N. (2001). Structure of the macrocycle thiostrepton solved using the anomalous dispersion contribution of sulfur. Acta Crystallogr. D Biol. Crystallogr. *57*, 755–758.
30. Varani, G., Aboul-ela, F., and Allain, F.H.-T. (1996). NMR investigation of RNA structure. Prog. NMR Spectrosc. *29*, 51–127.
31. Bissantz, C., Folkers, G., and Rognan, D. (2000). Protein-based virtual screening of chemical databases. 1. Evaluation of different docking/scoring combinations. J. Med. Chem. *43*, 4759–4767.
32. Bodley, J.W., Zieve, F.J., Lin, L., and Zieve, S.T. (1970). Studies on translocation. 3. Conditions necessary for the formation and detection of a stable ribosome-G factor-guanosine diphosphate complex in the presence of fusidic acid. J. Biol. Chem. *245*, 5656–5661.
33. Cundliffe, E., and Thompson, J. (1981). The mode of action of nosiheptide (multhiomycin) and the mechanism of resistance in the producing organism. J. Gen. Microbiol. *126*, 185–192.
34. Selva, E., Beretta, G., Montanini, N., Saddler, G.S., Gastaldo, L., Ferrari, P., Lorenzetti, R., Landini, P., Ripamonti, F., Goldstein, B.P., et al. (1991). Antibiotic GE2270A: a novel inhibitor of bacterial protein synthesis. I. Isolation and characterization. J. Antibiot. (Tokyo) *44*, 693–701.
35. Porse, B.T., Cundliffe, E., and Garrett, R.A. (1999). The antibiotic micrococcin acts on protein L11 at the ribosomal GTPase centre. J. Mol. Biol. *287*, 33–45.
36. Wilson, K.S., and Noller, H.F. (1998). Mapping the position of translational elongation factor EF-G in the ribosome by directed hydroxyl radical probing. Cell *92*, 131–139.
37. Agrawal, R.K., Linde, J., Sengupta, J., Nierhaus, K.H., and Frank, J. (2001). Localization of L11 protein on the ribosome and elucidation of its involvement in EF-G-dependent translocation. J. Mol. Biol. *311*, 777–787.
38. Stark, H., Rodnina, M.V., Wieden, H.J., van Heel, M., and Wintermeyer, W. (2000). Large-scale movement of elongation factor G and extensive conformational change of the ribosome during translocation. Cell *100*, 301–309.
39. Murchie, A.I.H., and Lentzen, G.F. (2001). Assay for identification of a test compound binding to a target RNA using a RNA-modifying enzyme. PCT Int. Appl. WO 0179543.
40. Kirillov, S.V., Makhno, V.I., Peshin, N.N., and Semenkov, I.U. (1978). Nature of the heterogeneity of 30S ribosomal subparticles in vitro. I. Effect of large centrifugal fields during 30S subparticle isolation on their capacity for codon-dependent tRNA binding. Mol. Biol. (Mosk.) *12*, 602–611.
41. Rodnina, M., and Wintermeyer, W. (1995). GTP consumption of elongation factor Tu during translation of heteropolymeric mRNAs. Proc. Natl. Acad. Sci. USA *92*, 1945–1949.
42. Borowski, C., Rodnina, M.V., and Wintermeyer, W. (1996). Truncated elongation factor G lacking the G domain promotes translocation of the 3′ end but not of the anticodon domain of peptidyl-tRNA. Proc. Natl. Acad. Sci. USA *93*, 4202–4206.
43. Savelsbergh, A., Matassova, N., Rodnina, M., and Wintermeyer, W. (2000). Role of domains 4 and 5 in elongation factor G functions on the ribosome. J. Mol. Biol. *300*, 951–961.
44. Zubay, G. (1973). In vitro synthesis of protein in microbial systems. Annu. Rev. Genet. *7*, 267–287.
45. Beckler, G.S., Thompson, D., and Van Oosbree, T. (1995). In vitro translation using rabbit reticulocyte lysate. Methods Mol. Biol. *37*, 215–232.
46. Price, S.R., Oubridge, C., Varani, G., and Nagai, K. (1998). Preparation of RNA:protein complexes for x-ray crystallography and NMR. In RNA:Protein Interactions, C.W.J. Smith, ed. (Oxford: Oxford University Press), pp. 37–74.
47. van Wezel, G.P., and Bibb, M.J. (1996). A novel plasmid vector that uses the glucose kinase gene (glkA) for the positive selection of stable gene disruptants in Streptomyces. Gene *182*, 229–230.
48. Bower, J., Drysdale, M., Hebdon, R., Jordan, A., Lentzen, G., Matassova, N., Murchie, A., Powles, J., and Roughley, S. (2003). Structure-based design of agents targeting the bacterial ribosome. Bioorg. Med. Chem. Lett. *13*, 2455–2458.

Accession Numbers

Coordinates for the model have been deposited in the Protein Data Bank under ID code 1oln.